Published in final edited form as:

Cancer Res. 2015 July 1; 75(13): 2749–2759. doi:10.1158/0008-5472.CAN-14-3476.

Tracking and Functional Characterization of Epithelial-Mesenchymal Transition and Mesenchymal Tumor Cells During Prostate Cancer Metastasis

Marcus Ruscetti[1,2], **Bill Quach**[2], **Eman L. Dadashian**[2], **David J. Mulholland**[2,^], and **Hong Wu**[1,2,3,*]

[1]Molecular Biology Institute, University of California, Los Angeles, California

[2]Department of Molecular and Medical Pharmacology, University of California, Los Angeles, California

[3]School of Life Sciences, Peking University, Beijing, China

Abstract

The epithelial-mesenchymal transition (EMT) has been postulated as a mechanism by which cancer cells acquire the invasive and stem-like traits necessary for distant metastasis. However, direct *in vivo* evidence for the role of EMT in the formation of cancer stem-like cells (CSC) and the metastatic cascade remains lacking. Here we report the first isolation and characterization of mesenchymal and EMT tumor cells, which harbor both epithelial and mesenchymal characteristics, in an autochthonous murine model of prostate cancer. By crossing the established *Pb-Cre*$^{+/-}$*;Pten*$^{L/L}$*;Kras*$^{G12D/+}$ prostate cancer model with a *vimentin-GFP* reporter strain, generating *CPKV* mice, we were able to isolate epithelial, EMT and mesenchymal cancer cells based on expression of vimentin and EpCAM. *CPKV* mice (but not mice with *Pten* deletion alone) exhibited expansion of cells with EMT (EpCAM^{+}/Vim-GFP^{+}) and mesenchymal (EpCAM^{-}/Vim-GFP^{+}) characteristics at the primary tumor site and in circulation. These EMT and mesenchymal tumor cells displayed enhanced stemness and invasive character compared to epithelial tumor cells. Moreover, they displayed an enriched tumor-initiating capacity and could regenerate epithelial glandular structures *in vivo*, indicative of epithelia-mesenchyme plasticity. Interestingly, while mesenchymal tumor cells could persist in circulation and survive in the lung following intravenous injection, only epithelial and EMT tumor cells could form macrometastases. Our work extends the evidence that mesenchymal and epithelial states in cancer cells contribute differentially to their capacities for tumor initiation and metastatic seeding, respectively, and that EMT tumor cells exist with plasticity that can contribute to multiple stages of the metastatic cascade.

*Corresponding author and contact information: Dr. Hong Wu, School of Life Sciences, Rm 106, Jin Guang Life Sciences Building, Peking University, No. 5 Yiheyuan Road, Beijing, China 100871, Phone: 86-10-6276-8720, hongwu@pku.edu.cn.

^Current address for D. Mulholland: Division of Hematology and Medical Oncology, Icahn School of Medicine, Mount Sinai Hospital, New York, New York.

Disclosure of Potential Conflicts of Interest: The authors do not have potential conflicts of interest.

Keywords

EMT; prostate cancer; mouse models; cancer stem cells; metastasis

Introduction

Prostate cancer is the most commonly diagnosed male malignancy and the second leading cause of cancer-related death in Western men (1). Although localized prostate cancer is treatable, metastatic, late stage castration-resistant prostate cancer (mCRPC) is currently incurable and represents the major cause of prostate cancer-related death (2). Recent studies have focused on the processes and pathway alterations that cause prostate tumor cells to disseminate and metastasize. We and others have shown that activation of the PI3K/AKT and RAS/MAPK pathways is associated with metastatic prostate cancer, and that activation of both pathways is sufficient to induce distant metastasis and an epithelial-mesenchymal transition (EMT) at the primary tumor site in genetically engineered mouse models (3–5). The acquisition of an EMT phenotype within localized cancer has been demonstrated to be sufficient to trigger lethal metastatic disease (4, 6, 7) and promote CRPC (8–10) in multiple model systems.

EMT, in the context of cancer, allows epithelial cancer cells to acquire migratory and invasive characteristics, as well as overcome senescence, apoptosis, and anoikis, properties that are essential for tumor cell dissemination and distant metastasis (11). Moreover, recent studies have also implicated EMT in the acquisition of stem-like qualities (12–14) and drug resistance properties (15). However, evidence for the role of EMT in cancer stem cell formation and metastasis is mostly based on either *in vitro* manipulation of cultured cell lines to induce EMT or the expression of EMT signature markers in human cancer samples (10). Therefore, a direct role for EMT in prostate tumor progression, dissemination of circulating tumor cells (CTCs) into the blood stream, and seeding of metastases at distant sites remains unclear due to the lack of *in vivo* models that recapitulate the metastatic process.

We previously reported that deletion of the *Pten* tumor suppressor gene and conditional activation of the $Kras^{G12D}$ oncogene in the murine prostate epithelium (Pb-$Cre^{+/-}$;$Pten^{L/L}$;$Kras^{G12D/+}$) leads to 100% penetrable macrometastasis to the lungs and liver, and an EMT phenotype at the primary tumor site (4). Although the Pb-$Cre^{+/-}$;$Pten^{L/L}$;$Kras^{G12D/+}$ (*CPK*) prostate cancer mouse model recapitulates late-stage, metastatic human prostate cancer and associates EMT with prostate cancer metastasis, whether tumor cells that have undergone an EMT contribute directly to tumor progression, dissemination, and distant macrometastasis has yet to be established. In this study, we develop an *in vivo* system that allows tracking of the dynamic EMT program and isolation of cells from the *CPK* prostate cancer model that have either completed (mesenchymal) or are transitioning through an EMT (EMT) for characterization and functional testing. Our *in vivo* analysis suggests that mesenchymal and epithelial states contribute to different stages of the prostate cancer disease, and that EMT tumor cells, which have the plasticity to readily

transition between epithelial and mesenchymal lineages, are able to contribute to multiple stages of the metastatic cascade.

Materials and Methods

Mouse strains

Vim-GFP reporter mice were purchased from GENSAT (16). After crossing *Vim-GFP* mice with the $Cre^{+/-};Pten^{L/L};Kras^{G/+}$ model (4), $Pb\text{-}Cre^{+/-};Pten^{L/L};Kras^{+/+};Vim\text{-}GFP$ male mice were crossed with $Pb\text{-}Cre^{-};Pten^{L/L};Kras^{G12D/+}$ female mice to generate the $Cre^{-};Pten^{L/L};Kras^{G/+};Vim\text{-}GFP$ (*V*), $Cre^{+/-};Pten^{L/L};Kras^{+/+};Vim\text{-}GFP$ (*CPV*), and $Cre^{+/-};Pten^{L/L};Kras^{G/+};Vim\text{-}GFP$ (*CPKV*) mouse models. These strains have been maintained on a mixed strain background. All studies with animals were performed under the regulation of the division of Laboratory Animal Medicine at the University of California at Los Angeles (UCLA).

Histology and immunohistochemistry

Immunohistochemistry (IHC) was performed on formalin-fixed, paraffin-embedded tissues. Antigen retrieval was performed by boiling sections in 10mM citrate buffer (pH6) for 30 minutes. The following primary antibodies were used: Vimentin (Cell Signaling; 5741), GFP (Cell Signaling; 2955), E-cadherin (BD Biosciences; 610181), P-S6 (Cell Signaling; 2215), PTEN (Cell Signaling; 9559), Ki67 (Vector Laboratories; VP-RM04), CK5 (Covance; PRB-160P), CK8 (Covance; MMS-162P), Synaptophysin (Dako; A0010), and Pan-Cytokeratin (Sigma; C1801).

Matrigel invasion assay

8μm transwell inserts (BD Biosciences) were coated with Matrigel (300 μg/ml) (BD Biosciences) and placed into 24-well culture plates. 5×10^4 sorted cells per population were resuspended in serum free media in the top chamber, while full serum media (Dulbecco's modified eagle medium (DMEM) with 10% Fetal Bovine Serum (FBS)) was used in the bottom chamber. 24 hours later, invaded cells were fixed with methanol, stained with 0.2% crystal violet, and counted using a light microscope at 10X magnification.

Matrigel sphere assay

The Matrigel sphere assay was carried out as previously described (18). 5×10^3 sorted cells from each cell population were plated in triplicate.

BrdU pulse labeling

BrdU pulse labeling was carried out as previously described (19). 2×10^4 FACS sorted cells per population were cytospun onto coated cytoslides (Thermo Scientific) at 500 rpm for 5 minutes using Cytospin4 (Thermo Scientific). Cells were fixed with 4% paraformaldehyde for 15 minutes, and stained with a BrdU (BD Biosciences; 563445) primary antibody. 10 fields per slide were counted at 20x magnification.

Subcutaneous tumor regeneration assay

Prostate lobes/regions from *CPKV* mice were separated as described (Fig. 3B), serrated, mixed with Matrigel, and transplanted subcutaneously into *NOD/SCID/IL2Rγ-null* (*NSG*) mice. Once tumors reached 2 cm in size, mice were euthanized, and tumors were again serrated, mixed with Matrigel, and passaged into new recipient hosts.

Orthotopic tumor regeneration assay

5×10^3 sorted cells per population were mixed in 50% Matrigel/media, loaded into a 10 μl Hamilton syringe (Microliter), and 2.5×10^3 cells were injected into each anterior lobe of the prostates of recipient *NSG* mice.

Tail vein injections

2.5×10^4 or 1×10^5 sorted cells from each population were resuspended in 200 μl of PBS and injected intravenously into *NSG* hosts. The presence of lung macrometastases was assessed by gross examination of formalin-fixed lung samples under a dissecting microscope.

Statistical analysis

Graphpad Prism software was used to calculate mean and standard deviation. Student's *t*-test was used to calculate the statistical significance between the two groups of data. $P < 0.05$ is considered significant.

Results

Tracking EMT and mesenchymal tumor cells in an endogenous prostate cancer model using a *Vimentin-GFP* reporter line

In order to generate an *in vivo* tracking system to study the role of EMT in prostate cancer progression and metastasis, we crossed *Vimentin-GFP* mice (16) with the *Pb-Cre*$^{+/-}$*;Pten*$^{L/L}$*;Kras*$^{G12D/+}$ (*CPK*) murine model of prostate cancer (4) we recently developed to create the *Pb-Cre*$^{+/-}$*;Pten*$^{L/L}$*;Kras*$^{G12D/+}$*;Vim-GFP* model (*CPKV*). *Vimentin-GFP* reporter mice, in which GFP expression is driven from the endogenous Vimentin promoter on a bacterial artificial chromosome (BAC) (16), were chosen because Vimentin is one of the earliest upregulated genes during the EMT process (21), and its expression is associated with high Gleason scores, disease recurrence, and bone metastasis in human prostate cancers (22, 23).

In 10–12 week old *CPKV* prostates, GFP staining overlaps with endogenous Vimentin expression, which marks EMT regions within the stromal compartment surrounding GFP-negative epithelial glandular structures (Fig. 1A). These EMT regions also contain cells that are PTEN$^-$ and P-S6$^+$, a surrogate marker for PTEN loss and activation of the PI3K pathway, confirming that these cells were originally derived from *Pten*$^{loxp/loxp}$ prostate epithelial cells that underwent Cre recombination (Fig. 1A). As it is possible that endogenous stromal cells in the prostate, including CD45$^+$ leukocytes, also express P-S6$^+$, we stained prostate sections from 4 week old *CPKV* mice, a time-point when these mice have not yet developed invasive prostate tumors or an EMT phenotype, to identify if

Vimentin$^+$/GFP$^+$ stromal cells in the prostate normally express P-S6$^+$. Indeed, Vimentin$^+$/GFP$^+$ stromal cells in these prostates were PTEN$^+$ and P-S6$^-$ (Supplementary Fig. S1A). Moreover, in WT *Vim-GFP* (V) prostates, all Vimentin$^+$/GFP$^+$ stromal cells are also P-S6$^-$ (Supplementary Fig. S1B). These results verify that P-S6 can be used as a marker in our *CPKV* model to distinguish Vimentin$^+$/GFP$^+$/PTEN$^+$ stromal cells from Vimentin$^+$/GFP$^+$/PTEN$^-$ EMT cells derived from the *Pten*$^{-/-}$ prostate epithelium.

In order to isolate and characterize tumor cells with epithelial and mesenchymal characteristics from the prostates of *CPKV* mice, a FACS gating strategy was designed in which the epithelial cell adhesion molecule (EpCAM) was used as an epithelial marker and GFP as a mesenchymal marker (Supplementary Fig. S1A). Cells from *CPKV* prostates were first negatively selected from CD45$^+$, CD31$^+$, and Ter119$^+$ fractions (referred to as Lin$^-$) in order to avoid contamination from leukocyte, endothelial, and erythrocyte populations, respectively, as these cell types are known to express Vimentin (21). While age-matched WT *Vim-GFP* (*V*) (n=8) and *Pb-Cre*$^{+/-}$;*Pten*$^{L/L}$;Vim-GFP (*CPV*) (n=8) mutant prostates have a very rare population of cells that are EpCAM$^-$/GFP$^+$, which we will refer to as mesenchymal tumor cells, *CPKV* mutants (n=13) have a significant induction of the mesenchymal tumor cell population by 10 weeks of age (Fig. 1B and Supplementary Fig. S1C). Interestingly, a significant population of cells that co-express both epithelial and mesenchymal markers (EpCAM$^+$GFP$^+$), hereafter referred to as EMT cells, could also be isolated from 10–12 week old *CPKV*, and, to a small extent, *CPV* prostates, but not *V* prostates (Fig. 1B and Supplementary Fig. S1C). While there was a marginal increase in the percentage of EpCAM$^+$GFP$^-$ epithelial cells within *CPV* and *CPKV* prostates compared to *V* prostates, this change was not significant (Fig. 1B and Supplementary Fig. S1A). Genomic PCR analysis confirmed that all three FACS isolated tumor cell populations were indeed derived from epithelial cells that initially underwent Cre recombination, as they exhibit *Pten* deletion and *Kras* activation (Supplementary Fig. S1D).

To assess the association of the EMT and mesenchymal tumor cell populations with prostate cancer progression, we compared 10–12 week old *CPKV* mutants (n=11), which have begun to develop poorly differentiated EMT morphology, to late stage 15–20 week old mutants (n=9) with sarcomatoid morphology (4). While there was a significant expansion of mesenchymal tumor cells during tumor progression, there was no change in the percentage of EMT tumor cells in the 15–20 week old mutants (Fig. 1C), indicating that EMT tumor cells may indeed represent a transition stage. Histologically, rare EMT tumor cells that co-expressed both epithelial (E-cadherin; red) and mesenchymal markers (Vim-GFP; Green) were found within epithelial acinar structures, indicating that the early steps of the EMT process do not occur exclusively along the leading edge of the tumor (Fig. 1D, yellow arrows).

Finally, we confirmed that EpCAM$^+$/GFP$^+$ and EpCAM$^-$/GFP$^+$ cell populations isolated from *CPKV* prostates indeed display EMT signature gene expression by qPCR analysis. While both EMT and mesenchymal tumor cells had induced expression of EMT signature genes compared to epithelial tumor cells, mesenchymal prostate tumor cells displayed more dramatically increased expression of the EMT transcription factors *Snail* and *Zeb1*, as well as a switch from E-cadherin (*Cdh1*) to N-cadherin (*Cdh2*) expression (Fig. 1E).

Mesenchymal tumor cells were also significantly more invasive *ex vivo* compared to epithelial tumor cells, with EMT tumor cells displaying an intermediate invasive capacity (Fig. 1F). Taken together, we have developed a novel system by using a *Vim-GFP* reporter to faithfully track the dynamics of the EMT program and to isolate and characterize cells undergoing or having undergone an EMT in an endogenous prostate cancer model.

EMT and mesenchymal tumor cells have enhanced stemness properties

To explore whether EMT and mesenchymal tumor cells from an endogenous prostate cancer model have enhanced stemness qualities, tumor cell populations from primary *CPKV* prostates were isolated by FACS and grown in Matrigel cultures to assess their ability to form spheres, an *in vitro* assay used to assess stemness characteristics (18). Indeed, EMT tumor cells could generate significantly more spheres than both epithelial and mesenchymal tumor cells (Fig. 2A). The EMT tumor cell subpopulation also contained a higher proportion of $Lin^{-}Sca1^{+}CD49f^{high}$ (LSC^{hi}) stem/progenitor cells (Fig. 2B), which have been previously shown to have a basal cell phenotype, high sphere-forming activity, and be sufficient to initiate tumorigenesis and metastasis (4, 24). These findings suggest that EMT tumor cells may represent a subpopulation of tumor cells with enhanced stemness qualities.

Compared to both epithelial and EMT tumor cell populations, mesenchymal tumor cells had reduced *in vitro* sphere-forming capacity (Fig. 2A). However, mesenchymal tumor cells had significantly increased expression of genes involved in maintenance of the stem cell state, including the *Sox* family members *Sox5*, *Sox9*, *Sox10*, and *Sox17*, the reprogramming factors *Klf2* and *Klf4*, the self-renewal maintenance factors *Bmi1*, *Nestin*, and *Lrig1*, and members of the WNT and NOTCH developmental pathways, suggesting that mesenchymal tumor cells may also harbor stemness qualities (Fig. 2C and 2D). One possible explanation for their poor sphere-forming capacity may be that mesenchymal tumor cells exist in a quiescent state and therefore have less capacity to proliferate and form sphere structures (25, 26). To test this hypothesis, we pulse labeled CPKV mice with 5-bromo-2′-deoxyuridine (BrdU) for 24 hours prior to FACS sorting to assess the percentage of cycling cells in each population. While the epithelial and EMT tumor cell populations had a high percentage of cells in S-phase, the mesenchymal tumor cell population had a much lower percentage of cycling cells (Fig. 2E). In support of this finding, our Ki67 immunohistochemical analysis revealed that E-cadherin-positive glandular structures are more proliferative than GFP-positive mesenchymal regions in the stroma (Fig. 2F). In summary, both EMT and mesenchymal tumor cells from *CPKV* mutants have enhanced stemness characteristics, with EMT tumor cells displaying a proliferative, stem/progenitor cell phenotype, and mesenchymal tumor cells exhibiting a quiescent stem cell phenotype.

Prostate regions enriched in Vim-GFP^{+} cells are able to regenerate transplantable tumors *in vivo*

As prostate stem cells have been previously shown to reside in the proximal region of the prostate attached to the urethra (25), we next wanted to ascertain if EMT and mesenchymal tumor cells were also enriched in this stem cell niche. Gross fluorescent imaging of whole *CPKV* prostates revealed that Vim-GFP expression was most prominent in the proximal anterior lobes, and, interestingly, in the anterior portion of the urethra itself (Fig. 3A). When

distinct anatomical regions of the prostate were separated from 10-week old *CPKV* mice with established tumors (Fig. 3B) and subjected to quantitative FACS analysis, the percentage of mesenchymal tumor cells was significantly higher in the proximal region of the anterior lobes and the anterior portion of the urethra, the regions immediately connected to the proximal region of the prostate, compared to other regions of *CPKV* prostates (Fig. 3C, right panel, n=3). Although the percentage of EMT tumor cells was slightly higher in the proximal region of anterior lobes, the percentage of EMT tumor cells did not change dramatically between the different regions of the prostate (Fig. 3C, left panel, n=3). This data suggests that mesenchymal tumor cells may indeed have properties of quiescent stem cells, which are localized to specific stem cell niches.

To test whether the regions of *CPKV* prostates with the highest percentage of EMT and mesenchymal tumor cells also have the highest tumor-initiating capacity, regions/lobes were separated from 10-week old *CPKV* prostates, mixed with matrigel, and implanted subcutaneously into *NOD/SCID/IL2Rγ-null* (*NSG*) mice. Remarkably, the only regions that were able to form subcutaneous tumors *in vivo* were from the proximal region of the anterior gland and anterior portion of the urethra, the same regions with the highest percentage of EMT and mesenchymal tumor cells (Fig. 3D, n=4). Tumors from both regions were able to be serially passaged, and these passaged tumors contained all 3 prostatic cell lineages ($CK5^+$ basal, $CK8^+$ luminal, and $Synaptophysin^+$ neuroendocrine cells) (Supplementary Fig. S2), demonstrating that stem cells within these regions have the capacity to regenerate all prostate lineages.

EMT and mesenchymal tumor cells have enhanced tumor-initiating capacity and cellular plasticity *in vivo*

In order to directly assess the tumor-initiating capacity of epithelial, EMT and mesenchymal tumor cells isolated from *CPKV* mice, 5,000 sorted cells from each population were implanted orthotopically into the anterior lobes of *NSG* mice and allowed to incubate up to 6 months (Fig. 4A). Tumor pathology was defined histologically by the presence of abnormal glandular structures, stromal expansion, and positive staining for P-S6 and Ki67, which should not be present in normal prostate tissue (Fig. 4C and 4D and Supplementary Fig. S3A). While EMT and mesenchymal tumor cells have a high tumor-initiating capacity *in vivo*, with 6/9 and 7/9 mice injected with these tumor cells forming prostate tumors, respectively, only 3/13 mice injected with epithelial tumor cells formed tumor pathology *in vivo* (Fig. 4B and Supplementary Fig. S3A). EMT and mesenchymal tumor cells also formed tumors as early as 9 weeks and 6 weeks post-transplantation, respectively, whereas the epithelial tumor cells did not form tumors until 24 weeks post-transplantation (Supplementary Fig. S3B). Tumorigenic areas formed from transplanted epithelial tumor cells were also much less aggressive compared to those formed by EMT and mesenchymal tumor cells (T; Supplementary Fig. S3A). EMT and mesenchymal tumor cells generated tumors with vast regions of EMT morphology that were positive for both Vimentin and P-S6 (Fig. 4C and 4D, bottom panels). Despite initially being injected as GFP^+ cells, EMT and mesenchymal tumor cells were also remarkably able to regenerate tumorous epithelial acinar structures with prostatic intraepithelial neoplasia (PIN) lesions that were Vimentin-negative and P-S6-positive (Fig. 4C and 4D, top panels), indicating that these cells have the plasticity

to switch between mesenchymal and epithelial states. In general, while regenerated epithelial glandular structures were positive for proliferation markers (Ki67), invasive EMT regions were devoid of any proliferation markers in tumors generated from EMT and mesenchymal tumor cells (Fig. 4C and 4D), mimicking the phenotype seen in primary *CPKV* prostates (Fig. 2F). These results demonstrate that EMT and mesenchymal tumor cells have enhanced tumor-initiating capacity compared to epithelial tumor cells from the same *CPKV* mice, and that these cells have an inherent plasticity to switch between mesenchymal and epithelial states, as they are able to form invasive tumor regions that are P-S6^{+}, Vimentin^{+}, and Ki67^{lo}, as well as regenerated glandular structures that are P-S6^{+}, Ki67$^{int/hi}$, and Vimentin^{-} (Fig. 4E).

Increase in CTCs with mesenchymal and invasive characteristics during disease progression in *CPKV* mice

Circulating tumor cells (CTCs) represent a surrogate biomarker of metastatic disease and a predictive factor of overall survival in various malignancies, including prostate cancer (27, 28). The current FDA-approved CellSearch method for CTC enumeration uses antibodies against EpCAM to isolate CTCs with epithelial characteristics (29). However, recent studies in human breast and prostate cancer patients have revealed that a significant percentage of CTCs co-express both mesenchymal and epithelial markers or display fully mesenchymal characteristics (23, 30–32), through which they could pass undetected by the CellSearch system.

To determine if we could use the *Vim-GFP* reporter to isolate and characterize CTCs with EMT and mesenchymal characteristics at different disease stages, we collected peripheral blood from *CPKV* mutants. CTCs were isolated and characterized from the Lin^{-} population by FACS analysis in a similar manner to how the primary tumor cell populations were isolated (Supplementary Fig. S4A). As early as 6 weeks of age and well before the detection of metastatic disease, epithelial, EMT and mesenchymal CTCs can be detected in the blood of *CPKV* mice (Fig. 5A, left panel, n=7). During the intermediate (10–12 weeks) and late stages (15–20 weeks) of tumor progression, there is a significant expansion of mesenchymal CTCs and rare EMT CTCs but not epithelial CTCs in *CPKV* mice, suggesting that only mesenchymal and EMT CTC counts correlate with progression towards metastatic disease (Fig. 5A, middle and right panels, n=10). Supporting this finding, *CPV* mice, which develop micrometastases in the lymph nodes but not distant macrometastasis to the lung or liver (33), show similar epithelial CTC numbers to age-matched *CPKV* mice but have very few CTCs with mesenchymal characteristics and no CTCs with EMT traits (Fig. 5A, n=5). This data suggests that 1) dissemination of metastatic tumor cells occurs early on during tumor initiation, 2) mesenchymal and EMT CTC counts correlate with metastatic disease, and 3) EMT tumor cells may quickly polarize to a mesenchymal or epithelial phenotype upon entering blood circulation.

As it is thought that disseminated cells with metastatic seeding potential must possess stem cell characteristics in order to colonize distant tissues, we looked at expression of CD44, a putative cancer stem cell (CSC) marker (34), in our different CTC subpopulations. Throughout the various stages of disease progression in *CPKV* mice, the majority of CTCs

with mesenchymal characteristics also expressed CD44, while only a small percentage of epithelial CTCs expressed this CSC marker (Fig. 5B, n=10). Interestingly, 100% of rare EMT CTCs that could be detected were $CD44^+$ (Fig. 5B, n=10).

To further assess metastatic seeding potential of the CTC subpopulations, blood from *CPKV* mutants, as well as *CPV* and *V* mutants, was incubated on Vitatex culture plates, which are coated with a cell-adhesion matrix (CAM) that is used to assess the ability of tumor cells to invade collagen matrices (20, 35). Utilizing a Vitatex plate coated with a fluorescent red CAM, we are able to identify invasive CTCs (iCTCs), which represent CTCs with metastatic potential, by their ability to invade through the matrix and ingest TRITC-labeled CAM (Supplementary Fig. S4B). After 10 days in culture, blood isolated from *CPKV* mice (n=10) had a significantly larger number of $TRITC^+$ iCTCs compared to blood from *CPV* (n=5) or *V* mice (n=3), supporting the notion that CTCs in *CPKV* mice contain more metastatic seeding potential (Fig. 5C). Moreover, when exploring the phenotype of these iCTCs from *CPKV* mice by FACS analysis, the majority of iCTCs had mesenchymal characteristics (Fig. 5D). The *Vim-GFP* reporter can therefore also be utilized for the isolation and characterization of CTC populations during endogenous prostate tumor cell dissemination and metastatic spreading. Our analysis reveals that *CPKV* mice have a significant increase in EMT and mesenchymal CTCs, but not epithelial CTCs, during disease progression.

Epithelial tumor cells have enhanced metastatic seeding potential

The observation that metastatic lesions in humans often display an epithelial morphology suggests that tumor cells that have disseminated through an EMT may revert to an epithelial phenotype through a mesenchymal-epithelial transition (MET) in order to form macrometastases (36). To test whether an MET may be required for macroscopic metastasis in *CPKV* mice, we compared epithelial and mesenchymal marker expression in both micrometastases, which remain small, dormant lesions, and actively proliferating macrometastases in the lungs. While micrometastases express high levels of Vimentin and low levels of Pan-Cytokeratin (CK) and Ki67, macrometastases express low levels of Vimentin and high levels of CK and Ki67 (Fig. 6A). This data suggests that a reversion to an epithelial phenotype, marked by high levels of CK, may be required for dormant micrometastases with mesenchymal features to proliferate to form macrometastases.

We next wanted to directly test the metastatic seeding capacity of epithelial, EMT and mesenchymal tumor cell populations by injecting these primary tumor cell populations isolated from *CPKV* mice intravenously into *NSG* mice. Remarkably, while mesenchymal tumor cells were unable to form macrometastases up to 16 weeks post-transplantation, epithelial tumor cells readily formed macrometases when either 25,000 (2/5) or 100,000 (6/6) tumor cells were injected (Fig. 6B and 6C). EMT tumor cells were also able to form metastases (1/5), albeit at a lower efficiency compared to epithelial tumor cells (Fig. 6B and 6C). Upon histological examination of the lungs post-transplantation, the macrometastases formed by both epithelial and EMT tumor cells were devoid of GFP^+ cells and expressed high levels of CK (Supplementary Fig. S5), similar to lung macrometastases found in *CPKV* mice (Fig. 6A), confirming that macrometastatic spread requires reversion to an epithelial phenotype. While mesenchymal tumor cells did not form macrometastases or even small

micrometastases in the lungs, solitary GFP^+ cells were found in a quiescent, non-proliferative state ($Ki67^-$) throughout the lungs (Supplementary Fig. S5). Interestingly, while few tumor cells remained in the circulation of mice transplanted with epithelial and EMT tumor cells 16 weeks post-intravenous injection, those transplanted with mesenchymal tumor cells had a significantly high number of CTCs with mesenchymal characteristics, suggesting that mesenchymal cells can persist and survive in the blood stream for long periods of time (Fig. 6D, n=4). These findings propose that while mesenchymal tumor cells are able to survive in the blood, extravasate, and persist as solitary, dormant cells in the lungs over the course of 16 weeks, they are unable to proliferate to generate frank metastases. EMT tumor cells, on the other hand, reside in a transitionary state, and have the capacity to transition to an epithelial state in order to proliferate and form macrometastases. Overall, while both EMT and mesenchymal prostate tumor cells have enhanced stemness characteristics and tumor-initiating capacity compared to epithelial tumor cells, only EMT tumor cells have the capacity to revert to an epithelial state and proliferate in the lungs to form macrometastases (Fig. 6E).

Discussion

As EMT is a plastic and dynamic process, the study of the EMT process through the *in vitro* manipulation of established cell lines, which often polarizes cells into a fixed mesenchymal state, may overlook much of the biology involved within the transition. Here, we demonstrate for the first time the isolation and characterization of both mesenchymal tumor cells that have fully completed an EMT, as well as EMT tumor cells that are in a transitory state between epithelial and mesenchymal programs from an endogenous murine cancer model. While previous studies have suggested that partial but not complete passage of cells into a mesenchymal state is associated with stemness and tumorigenicity (17, 37, 38), our study reveals that both EMT and mesenchymal tumors cells harbor stemness characteristics and tumor-initiating capacity. A striking distinction between these populations is their proliferative capacity, with mesenchymal tumor cells exhibiting characteristics of quiescent stem cells, and EMT tumor cells exhibiting characteristics of proliferating progenitor cells. Given that mesenchymal tumor cells localize to the stem cell niche in the proximal region of the prostate, it is likely that they are maintained in a quiescent state by factors in the surrounding microenvironment (26).

While both EMT and mesenchymal tumor cells demonstrate the plasticity to initiate proliferative epithelial tumor structures in the prostate microenvironment, only EMT cells are able to quickly revert to an epithelial phenotype to form macrometastatic colonies in the lungs. This suggests that mesenchymal tumor cells may exist in a more fixed state compared to EMT tumor cells, and may require additional stimuli, possibly mediated through paracrine factors secreted from the surrounding microenvironment, in order to acquire an epithelial phenotype and proliferate to form distant metastases. The modeling of dissemination in immunodeficient mice in our study, as well as by others (17, 39), presents a number of caveats that may affect the rate of successful metastatic colonization. First, *NSG* mice lack mature T cells, B cells, and NK cells, and have documented defects in macrophage activation. This is problematic, as the outgrowth of macrometastases has been shown to rely on the successful recruitment of myeloid and other inflammatory cell types to

the metastatic site (40). Second, primary tumors release systemic factors that can educate distant sites in preparation for metastasizing cancer cells and mobilize bone marrow-derived cells to these sites to orchestrate what is termed the “premetastatic niche” (41–43). The lack of both a primary tumor and various immune cell subtypes in our dissemination model may indeed impact the metastatic niche required for colonization. Future studies exploring the contribution of distinct tumor cell populations to metastatic colonization will need to be carried out using lineage-tracing techniques in endogenous mouse models or through transplantation of tumor cells into immunocompetent syngeneic mice to fully recapitulate the role of the tumor microenvironment in metastatic colonization. Finally, as human prostate cancer metastasizes most frequently to the bone, it is plausible that the mesenchymal state, as opposed to the epithelial state, may be favored for metastatic colonization in the bone microenvironment. Indeed, a number of studies have demonstrated that human prostate cancer bone metastases have downregulation of E-cadherin and increased mesenchymal marker expression (44–47).

Given that mesenchymal CTCs increase in number significantly during disease progression in *CPKV* mice and harbor stemness properties, it is likely that mesenchymal tumor cells can settle in the distant organ sites and eventually form macrometastases, albeit over long latency periods. It has been well documented in the clinic that disseminated tumor cells (DTCs) can persist in a quiescent state at metastatic sites for decades after surgical removal of the primary tumor and eventually give rise to macrometastases (48, 49). It is possible that disseminated mesenchymal tumor cells in our *CPKV* mice model the clinical phenomenon of metastatic dormancy, and that the observation window of our metastasis assay (16 weeks) was not long enough to observe reactivation of these dormant, solitary DTCs to produce growing macrometastases. Moreover, while epithelial tumor cells can readily form metastases in the lung after entering the blood stream, it is unlikely that they can actively disseminate from the primary tumor in the endogenous setting. However, we cannot rule out the possibility that epithelial and mesenchymal tumor cells dynamically interact at different stages of the invasion-metastasis cascade to produce macrometastatic disease (17, 39). On the other hand, EMT tumor cells, by harboring the plasticity to readily transition between epithelial and mesenchymal states, have the capacity to complete the entirety of the invasion-metastasis cascade on their own. A preliminary transcriptional profiling study of each cell population revealed significant alterations in a number of key epigenetic regulators in the EMT and mesenchymal tumor cell populations, including HMGA2, which we found to be 1) significantly upregulated in human mCRPC, 2) required for epithelial-mesenchymal plasticity, and 3) successfully targeted by the histone deacteylase inhibitor (HDACi) LBH589 for therapeutic benefit *in vivo* (data in preparation). While more detailed analyses are warranted and still ongoing, these findings provide strong support for the use of therapeutic agents that target prostate tumor cell plasticity, as opposed to therapies that specifically target the epithelial or mesenchymal state. Although therapeutic targeting of mesenchymal tumor cells and the mesenchymal state could be useful in preventing tumor progression and dissemination, such therapeutic strategies could be counterproductive in patients that have DTCs or dormant micrometastases, since promoting reversion to an epithelial state could in turn promote metastatic growth. Further understanding of the mechanisms regulating epithelial-mesenchymal plasticity will help to unveil novel therapies

that can be used to target tumor cell plasticity and hence inhibit integral steps of the metastastic cascade that ultimately leads to prostate cancer mortality.

Supplementary Material

Refer to Web version on PubMed Central for supplementary material.

Acknowledgments

Grant Support:

MR was supported by NIH T32 CA009056. DJM was supported by NIH F32 CA112988-01, CIRM TG2-01169 and Prostate Cancer Foundation Young Investigator Award. This work has been supported in part by awards from the Prostate Cancer Foundation, and grants from the NIH (R01 CA107166, RO1 CA121110, P50 CA092131 and U01 CA164188 to HW).

The authors thank members of the Hong Wu lab for their critical comments and suggestions. We also thank Naoko Kobayashi, Antreas Hindoyan, and Diana Moughon for their technical assistance.

References

1. Siegel R, Ma J, Zou Z, Jemal A. Cancer statistics, 2014. CA: a cancer journal for clinicians. 2014; 64:9–29. [PubMed: 24399786]
2. Heidenreich A, Pfister D, Merseburger A, Bartsch G. Castration-resistant prostate cancer: where we stand in 2013 and what urologists should know. European urology. 2013; 64:260–5. [PubMed: 23706522]
3. Taylor BS, Schultz N, Hieronymus H, Gopalan A, Xiao Y, Carver BS, et al. Integrative genomic profiling of human prostate cancer. Cancer cell. 2010; 18:11–22. [PubMed: 20579941]
4. Mulholland DJ, Kobayashi N, Ruscetti M, Zhi A, Tran LM, Huang J, et al. Pten loss and RAS/MAPK activation cooperate to promote EMT and metastasis initiated from prostate cancer stem/progenitor cells. Cancer research. 2012; 72:1878–89. [PubMed: 22350410]
5. Aytes A, Mitrofanova A, Kinkade CW, Lefebvre C, Lei M, Phelan V, et al. ETV4 promotes metastasis in response to activation of PI3-kinase and Ras signaling in a mouse model of advanced prostate cancer. Proceedings of the National Academy of Sciences of the United States of America. 2013; 110:E3506–15. [PubMed: 23918374]
6. Lue HW, Yang X, Wang R, Qian W, Xu RZ, Lyles R, et al. LIV-1 promotes prostate cancer epithelial-to-mesenchymal transition and metastasis through HB-EGF shedding and EGFR-mediated ERK signaling. PloS one. 2011; 6:e27720. [PubMed: 22110740]
7. Josson S, Nomura T, Lin JT, Huang WC, Wu D, Zhau HE, et al. beta2-microglobulin induces epithelial to mesenchymal transition and confers cancer lethality and bone metastasis in human cancer cells. Cancer research. 2011; 71:2600–10. [PubMed: 21427356]
8. Tanaka H, Kono E, Tran CP, Miyazaki H, Yamashiro J, Shimomura T, et al. Monoclonal antibody targeting of N-cadherin inhibits prostate cancer growth, metastasis and castration resistance. Nature medicine. 2010; 16:1414–20.
9. Sun Y, Wang BE, Leong KG, Yue P, Li L, Jhunjhunwala S, et al. Androgen deprivation causes epithelial-mesenchymal transition in the prostate: implications for androgen-deprivation therapy. Cancer research. 2012; 72:527–36. [PubMed: 22108827]
10. Nauseef JT, Henry MD. Epithelial-to-mesenchymal transition in prostate cancer: paradigm or puzzle? Nature reviews Urology. 2011; 8:428–39.
11. De Craene B, Berx G. Regulatory networks defining EMT during cancer initiation and progression. Nature reviews Cancer. 2013; 13:97–110.
12. Mani SA, Guo W, Liao MJ, Eaton EN, Ayyanan A, Zhou AY, et al. The epithelial-mesenchymal transition generates cells with properties of stem cells. Cell. 2008; 133:704–15. [PubMed: 18485877]

13. Morel AP, Lievre M, Thomas C, Hinkal G, Ansieau S, Puisieux A. Generation of breast cancer stem cells through epithelial-mesenchymal transition. PloS one. 2008; 3:e2888. [PubMed: 18682804]
14. Giannoni E, Bianchini F, Masieri L, Serni S, Torre E, Calorini L, et al. Reciprocal activation of prostate cancer cells and cancer-associated fibroblasts stimulates epithelial-mesenchymal transition and cancer stemness. Cancer research. 2010; 70:6945–56. [PubMed: 20699369]
15. Marin-Aguilera M, Codony-Servat J, Reig O, Lozano JJ, Fernandez PL, Pereira MV, et al. Epithelial-to-mesenchymal transition mediates docetaxel resistance and high risk of relapse in prostate cancer. Molecular cancer therapeutics. 2014; 13:1270–84. [PubMed: 24659820]
16. Gong S, Zheng C, Doughty ML, Losos K, Didkovsky N, Schambra UB, et al. A gene expression atlas of the central nervous system based on bacterial artificial chromosomes. Nature. 2003; 425:917–25. [PubMed: 14586460]
17. Celia-Terrassa T, Meca-Cortes O, Mateo F, de Paz AM, Rubio N, Arnal-Estape A, et al. Epithelial-mesenchymal transition can suppress major attributes of human epithelial tumor-initiating cells. The Journal of clinical investigation. 2012; 122:1849–68. [PubMed: 22505459]
18. Lukacs RU, Goldstein AS, Lawson DA, Cheng D, Witte ON. Isolation, cultivation and characterization of adult murine prostate stem cells. Nature protocols. 2010; 5:702–13.
19. Garcia AJ, Ruscetti M, Arenzana TL, Tran LM, Bianci-Frias D, Sybert E, et al. Pten Null Prostate Epithelium Promotes Localized Myeloid-Derived Suppressor Cell Expansion and Immune Suppression during Tumor Initiation and Progression. Molecular and cellular biology. 2014; 34:2017–28. [PubMed: 24662052]
20. Friedlander TW, Ngo VT, Dong H, Premasekharan G, Weinberg V, Doty S, et al. Detection and characterization of invasive circulating tumor cells derived from men with metastatic castration-resistant prostate cancer. International journal of cancer Journal international du cancer. 2014; 134:2284–93. [PubMed: 24166007]
21. Satelli A, Li S. Vimentin in cancer and its potential as a molecular target for cancer therapy. Cellular and molecular life sciences : CMLS. 2011; 68:3033–46. [PubMed: 21637948]
22. Zhang Q, Helfand BT, Jang TL, Zhu LJ, Chen L, Yang XJ, et al. Nuclear factor-kappaB-mediated transforming growth factor-beta-induced expression of vimentin is an independent predictor of biochemical recurrence after radical prostatectomy. Clinical cancer research : an official journal of the American Association for Cancer Research. 2009; 15:3557–67. [PubMed: 19447876]
23. Armstrong AJ, Marengo MS, Oltean S, Kemeny G, Bitting RL, Turnbull JD, et al. Circulating tumor cells from patients with advanced prostate and breast cancer display both epithelial and mesenchymal markers. Molecular cancer research : MCR. 2011; 9:997–1007. [PubMed: 21665936]
24. Mulholland DJ, Xin L, Morim A, Lawson D, Witte O, Wu H. Lin-Sca-1+CD49fhigh stem/progenitors are tumor-initiating cells in the Pten-null prostate cancer model. Cancer research. 2009; 69:8555–62. [PubMed: 19887604]
25. Tsujimura A, Koikawa Y, Salm S, Takao T, Coetzee S, Moscatelli D, et al. Proximal location of mouse prostate epithelial stem cells: a model of prostatic homeostasis. The Journal of cell biology. 2002; 157:1257–65. [PubMed: 12082083]
26. Salm SN, Burger PE, Coetzee S, Goto K, Moscatelli D, Wilson EL. TGF-{beta} maintains dormancy of prostatic stem cells in the proximal region of ducts. The Journal of cell biology. 2005; 170:81–90. [PubMed: 15983059]
27. Scher HI, Jia X, de Bono JS, Fleisher M, Pienta KJ, Raghavan D, et al. Circulating tumour cells as prognostic markers in progressive, castration-resistant prostate cancer: a reanalysis of IMMC38 trial data. The lancet oncology. 2009; 10:233–9. [PubMed: 19213602]
28. de Bono JS, Scher HI, Montgomery RB, Parker C, Miller MC, Tissing H, et al. Circulating tumor cells predict survival benefit from treatment in metastatic castration-resistant prostate cancer. Clinical cancer research : an official journal of the American Association for Cancer Research. 2008; 14:6302–9. [PubMed: 18829513]
29. Riethdorf S, Fritsche H, Muller V, Rau T, Schindlbeck C, Rack B, et al. Detection of circulating tumor cells in peripheral blood of patients with metastatic breast cancer: a validation study of the

CellSearch system. Clinical cancer research : an official journal of the American Association for Cancer Research. 2007; 13:920–8. [PubMed: 17289886]

30. Yu M, Bardia A, Wittner BS, Stott SL, Smas ME, Ting DT, et al. Circulating breast tumor cells exhibit dynamic changes in epithelial and mesenchymal composition. Science. 2013; 339:580–4. [PubMed: 23372014]
31. Chen CL, Mahalingam D, Osmulski P, Jadhav RR, Wang CM, Leach RJ, et al. Single-cell analysis of circulating tumor cells identifies cumulative expression patterns of EMT-related genes in metastatic prostate cancer. The Prostate. 2013; 73:813–26. [PubMed: 23280481]
32. Kallergi G, Papadaki MA, Politaki E, Mavroudis D, Georgoulias V, Agelaki S. Epithelial to mesenchymal transition markers expressed in circulating tumour cells of early and metastatic breast cancer patients. Breast cancer research : BCR. 2011; 13:R59. [PubMed: 21663619]
33. Wang S, Gao J, Lei Q, Rozengurt N, Pritchard C, Jiao J, et al. Prostate-specific deletion of the murine Pten tumor suppressor gene leads to metastatic prostate cancer. Cancer cell. 2003; 4:209–21. [PubMed: 14522255]
34. Tang DG, Patrawala L, Calhoun T, Bhatia B, Choy G, Schneider-Broussard R, et al. Prostate cancer stem/progenitor cells: identification, characterization, and implications. Molecular carcinogenesis. 2007; 46:1–14. [PubMed: 16921491]
35. Lu J, Fan T, Zhao Q, Zeng W, Zaslavsky E, Chen JJ, et al. Isolation of circulating epithelial and tumor progenitor cells with an invasive phenotype from breast cancer patients. International journal of cancer Journal international du cancer. 2010; 126:669–83. [PubMed: 19662651]
36. Chaffer CL, Weinberg RA. A perspective on cancer cell metastasis. Science. 2011; 331:1559–64. [PubMed: 21436443]
37. Battula VL, Evans KW, Hollier BG, Shi Y, Marini FC, Ayyanan A, et al. Epithelial-mesenchymal transition-derived cells exhibit multilineage differentiation potential similar to mesenchymal stem cells. Stem Cells. 2010; 28:1435–45. [PubMed: 20572012]
38. Shamir ER, Pappalardo E, Jorgens DM, Coutinho K, Tsai WT, Aziz K, et al. Twist1-induced dissemination preserves epithelial identity and requires E-cadherin. The Journal of cell biology. 2014; 204:839–56. [PubMed: 24590176]
39. Tsuji T, Ibaragi S, Shima K, Hu MG, Katsurano M, Sasaki A, et al. Epithelial-mesenchymal transition induced by growth suppressor p12CDK2-AP1 promotes tumor cell local invasion but suppresses distant colony growth. Cancer research. 2008; 68:10377–86. [PubMed: 19074907]
40. Joyce JA, Pollard JW. Microenvironmental regulation of metastasis. Nature reviews Cancer. 2009; 9:239–52.
41. Psaila B, Lyden D. The metastatic niche: adapting the foreign soil. Nature reviews Cancer. 2009; 9:285–93.
42. Kaplan RN, Riba RD, Zacharoulis S, Bramley AH, Vincent L, Costa C, et al. VEGFR1-positive haematopoietic bone marrow progenitors initiate the pre-metastatic niche. Nature. 2005; 438:820–7. [PubMed: 16341007]
43. Hiratsuka S, Watanabe A, Aburatani H, Maru Y. Tumour-mediated upregulation of chemoattractants and recruitment of myeloid cells predetermines lung metastasis. Nature cell biology. 2006; 8:1369–75.
44. Umbas R, Schalken JA, Aalders TW, Carter BS, Karthaus HF, Schaafsma HE, et al. Expression of the cellular adhesion molecule E-cadherin is reduced or absent in high-grade prostate cancer. Cancer research. 1992; 52:5104–9. [PubMed: 1516067]
45. Sethi S, Macoska J, Chen W, Sarkar FH. Molecular signature of epithelial-mesenchymal transition (EMT) in human prostate cancer bone metastasis. American journal of translational research. 2010; 3:90–9. [PubMed: 21139809]
46. Lang SH, Hyde C, Reid IN, Hitchcock IS, Hart CA, Bryden AA, et al. Enhanced expression of vimentin in motile prostate cell lines and in poorly differentiated and metastatic prostate carcinoma. The Prostate. 2002; 52:253–63. [PubMed: 12210485]
47. Kwok WK, Ling MT, Lee TW, Lau TC, Zhou C, Zhang X, et al. Up-regulation of TWIST in prostate cancer and its implication as a therapeutic target. Cancer research. 2005; 65:5153–62. [PubMed: 15958559]

48. Giancotti FG. Mechanisms governing metastatic dormancy and reactivation. Cell. 2013; 155:750–64. [PubMed: 24209616]

49. Aguirre-Ghiso JA. Models, mechanisms and clinical evidence for cancer dormancy. Nature reviews Cancer. 2007; 7:834–46.

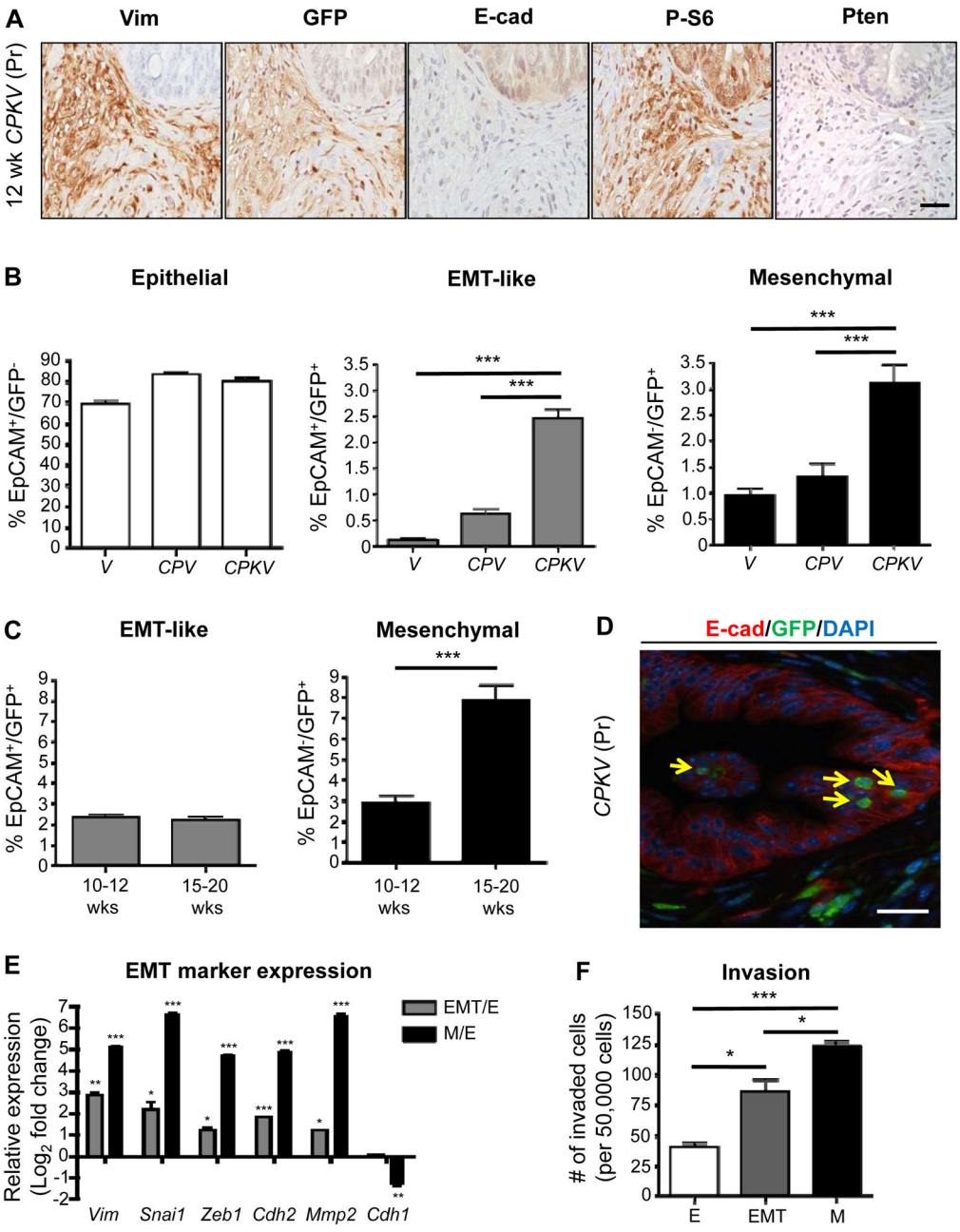

Figure 1.

Tracking EMT and mesenchymal tumor cells in an endogenous prostate cancer model using a *Vimentin-GFP* reporter line. **A**, Prostates from *CPKV* mice (12 weeks) display EMT regions that are Vimentin (Vim)/GFP-positive surrounding E-cadherin (E-cad)-positive epithelial glandular structures. P-S6 marks cells that have undergone Cre recombination. **B**, Vimentin-GFP (GFP) and EpCAM were used to characterize epithelial ($EpCAM^+/GFP^-$), EMT ($EpCAM^+/GFP^+$), and mesenchymal ($EpCAM^-/GFP^+$) cell populations from the prostates of various *Vim-GFP* reporter mice (10–12 weeks) by FACS. *CPKV* mice have significant expansion of EMT and mesenchymal tumor cell populations. **C**, Expansion of

mesenchymal tumor cell populations in *CPKV* prostates during late stage tumor progression (15–20 weeks). **D**, EMT cells (yellow arrow) that are GFP^+ (green) and E-cadherin $(E\text{-cad})^+$ (red) are found within epithelial glandular structures in *CPKV* prostates (12 weeks). **E**, qPCR analysis confirms EMT signature gene expression in EMT and mesenchymal tumor cells isolated from *CPKV* prostates (10–12 weeks). **F**, Matrigel invasion assay reveals that EMT and mesenchymal tumor cells isolated from *CPKV* prostates (10–12 weeks) are significantly more invasive than epithelial tumor cells. Data in B, C, E, and F are represented as mean ± SEM. Bar, 50 μm. Pr, prostate. Lin^-,$CD45^-/CD31^-/Ter119^-$. *, $P < 0.05$, **, $P < 0.01$. ***, $P < 0.001$.

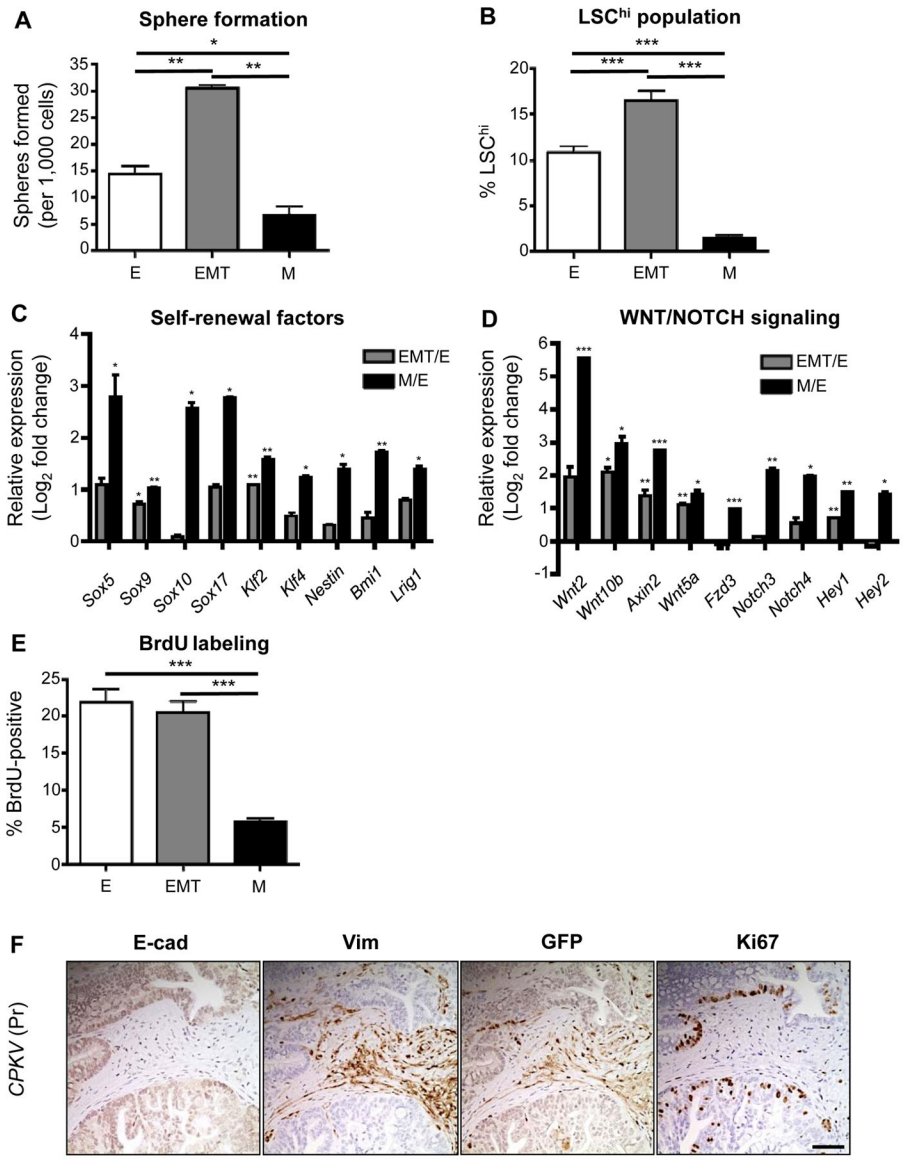

Figure 2.

EMT and mesenchymal tumor cells have enhanced stemness properties. **A**, Matrigel sphere assay reveals that EMT tumor cells sorted from *CPKV* prostates (10–12 weeks) form more spheres than epithelial and mesenchymal tumor cells after 7 days in culture. **B**, EMT tumor cells have a higher LSC^{hi} content compared to epithelial and mesenchymal tumor cells from *CPKV* prostates (10–12 weeks), as quantified by FACS. **C**, EMT and mesenchymal tumor cells from *CPKV* prostates (10–12 weeks) have enhanced expression of self-renewal and stemness factors compared to epithelial cells. **D**, EMT and mesenchymal tumor cells from *CPKV* prostates (10–12 weeks) have enhanced expression of genes involved in WNT and NOTCH signaling compared to epithelial cells. **E**, Epithelial and EMT tumor cells from *CPKV* prostates (10–12 weeks) have a higher percentage of cells in S-phase compared to mesenchymal tumor cells, as measured by the percentage of $BrdU^{+}$ cells. **F**, Ki67-positive cells are found preferentially in E-cadherin (E-cad)-positive glandular structures compared

to Vimentin (Vim)/GFP-positive EMT regions in the stroma of *CPKV* prostates (12 weeks). Data in A through E are represented as mean ± SEM. Bar, 100 μm. Pr, prostate. *, $P < 0.05$, **, $P < 0.01$. ***, $P < 0.001$.

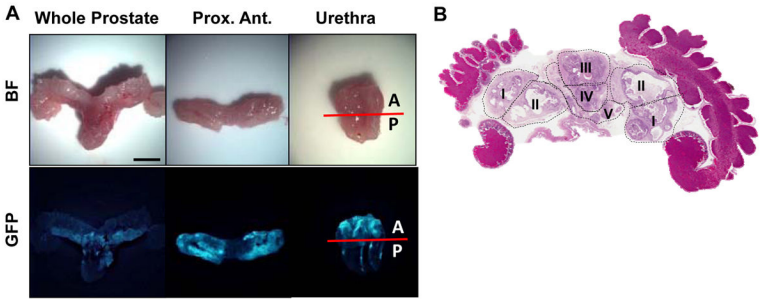

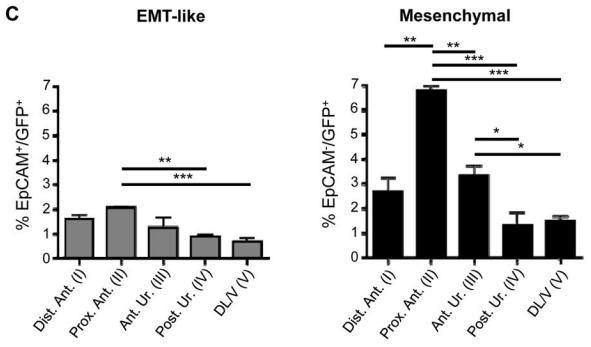

D

Prostate Lobes	P0	P1	P2	P3
Dist. Anterior (I)	-	-	-	-
Prox. Anterior (II)	+	+	+	+
Ant. Urethra (III)	+	+	+	+
Post. Urethra (IV)	-	-	-	-
Dorsolateral/ Ventral (V)	-	-	-	-

Figure 3.

Prostate regions enriched in Vim-GFP$^+$ cells are able to regenerate transplantable tumors *in vivo*. **A**, Bright-field (BF) and fluorescent images of a whole-mount *CPKV* prostate (10 weeks). GFP expression in *CPKV* prostates is most prominent in the proximal region of the anterior lobes and in the anterior portion of the urethra. **B**, Diagram depicting how prostate regions/lobes were separated. I, distal region of the anterior lobe. II, proximal region of the anterior lobe. III, anterior portion of the urethra. IV, posterior portion of the urethra. V, dorsolateral/ventral lobes. **C**, FACS analysis demonstrates that the anterior portion of the urethra and proximal region of the anterior lobes express the highest percentage of mesenchymal cells compared to other regions/lobes from the prostates of *CPKV* mice (10–12 weeks). The percentage of EMT tumor cells was also slightly higher in the proximal region of the anterior lobes compared to other lobes/regions. **D**, The only *CPKV* prostate regions/lobes that produced transplantable tumors in *NSG* mice were the proximal region of the anterior lobe and anterior portion of the urethra. Data in C are represented as mean ± SEM. Bar, 4mm. A, anterior. P, posterior. Dist. Ant., distal region of the anterior lobe. Prox. Ant., proximal region of the anterior lobe. Ant. Ur., anterior portion of the urethra. Post. Ur., posterior portion of the urethra. DL/V, dorsolateral/ventral lobes. P0, passage 0. P1, passage

1. P2, passage 2. P3, passage 3. +, tumor. −, no tumor. *, $P < 0.05$, **, $P < 0.01$. ***, $P < 0.001$.

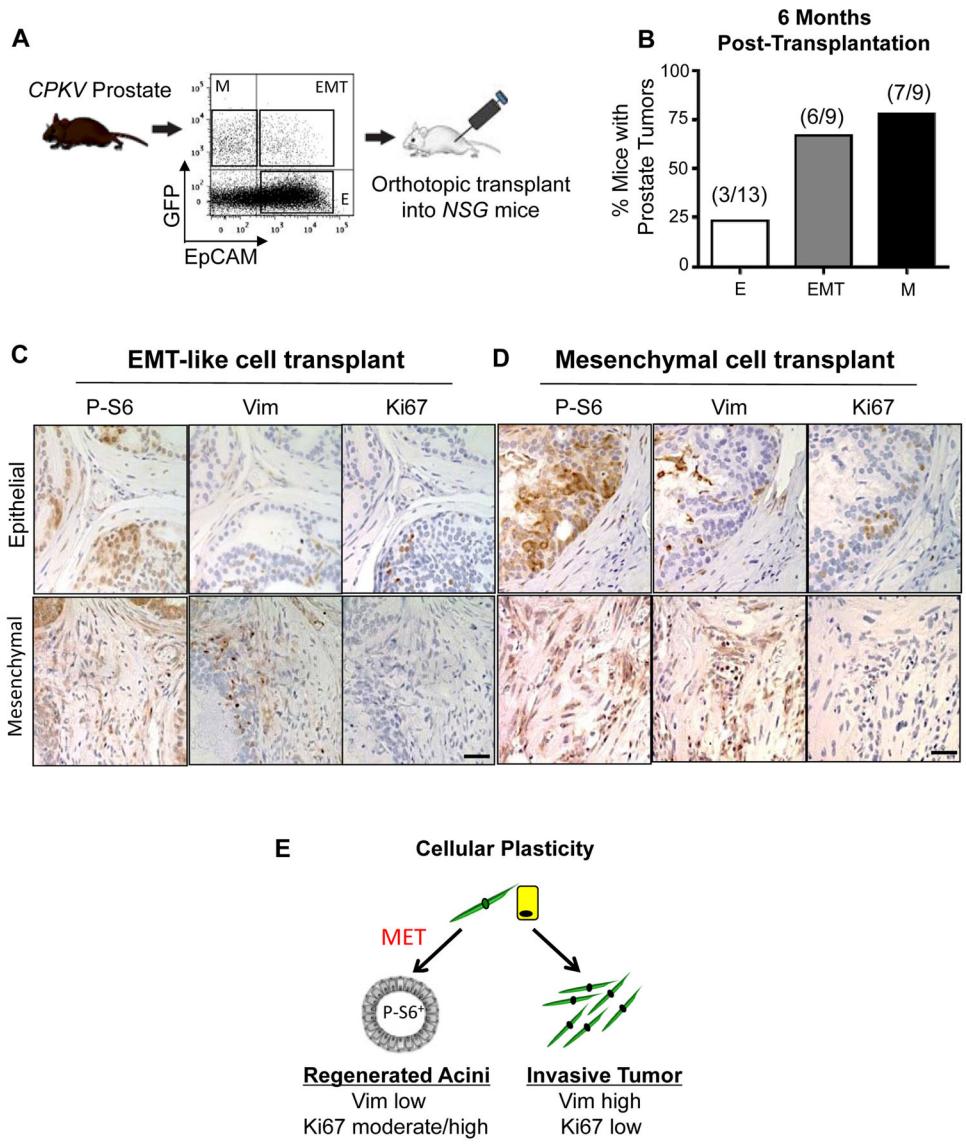

Figure 4.

EMT and mesenchymal tumor cells have enhanced tumor-initiating capacity and cellular plasticity *in vivo*. **A**, Schematic of experimental design for orthotopic transplantations. **B**, EMT and mesenchymal tumor cells form tumors more readily *in vivo* compared to epithelial tumor cells from *CPKV* prostates (10–12 weeks). **C**, IHC stains of anterior lobes from an *NSG* mouse transplanted with EMT tumor cells from *CPKV* prostates (10–12 weeks). P-S6 was used to trace transplanted cells, and Vim was used to mark mesenchymal cells. Top panel, transplanted EMT tumor cells form regenerated glandular structures. Bottom panel, transplanted EMT tumor cells form invasive mesenchymal tumor regions. **D**, Same as in C, except a prostate section from an *NSG* mouse transplanted with mesenchymal tumor cells from *CPKV* prostates (10–12 weeks). **E**, EMT (yellow) and mesenchymal (green) tumor cells from *CPKV* prostates have the plasticity to undergo an MET and regenerate epithelial glandular structures, or form invasive mesenchymal tumors *in vivo*. Bar, 50 μm.

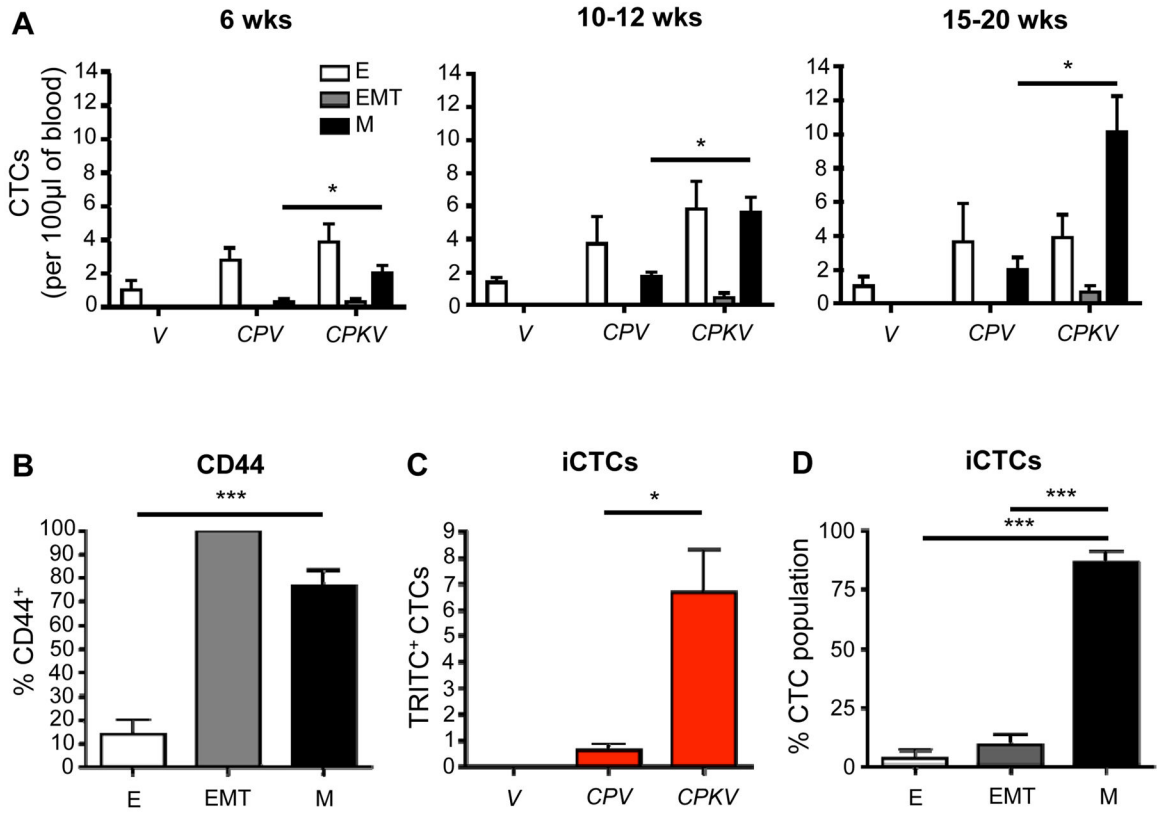

Figure 5.

Increase in CTCs with mesenchymal and invasive characteristics during disease progression in *CPKV* mice. **A**, *CPKV* mice have a significant increase in mesenchymal and EMT CTCs compared to *CPV* or *V* mice during disease progression. **B**, Mesenchymal and EMT CTCs from *CPKV* mice (15–20 weeks) have significantly higher CD44 expression compared to epithelial CTCs. **C**, *CPKV* mice have significantly more invasive CTCs (iCTCs) compared to *CPV* and *V* mice (15–20 weeks). **D**, The majority of iCTCs have a mesenchymal phenotype. Data in A through D are represented as mean ± SEM. *, $P < 0.05$, ***, $P < 0.001$.

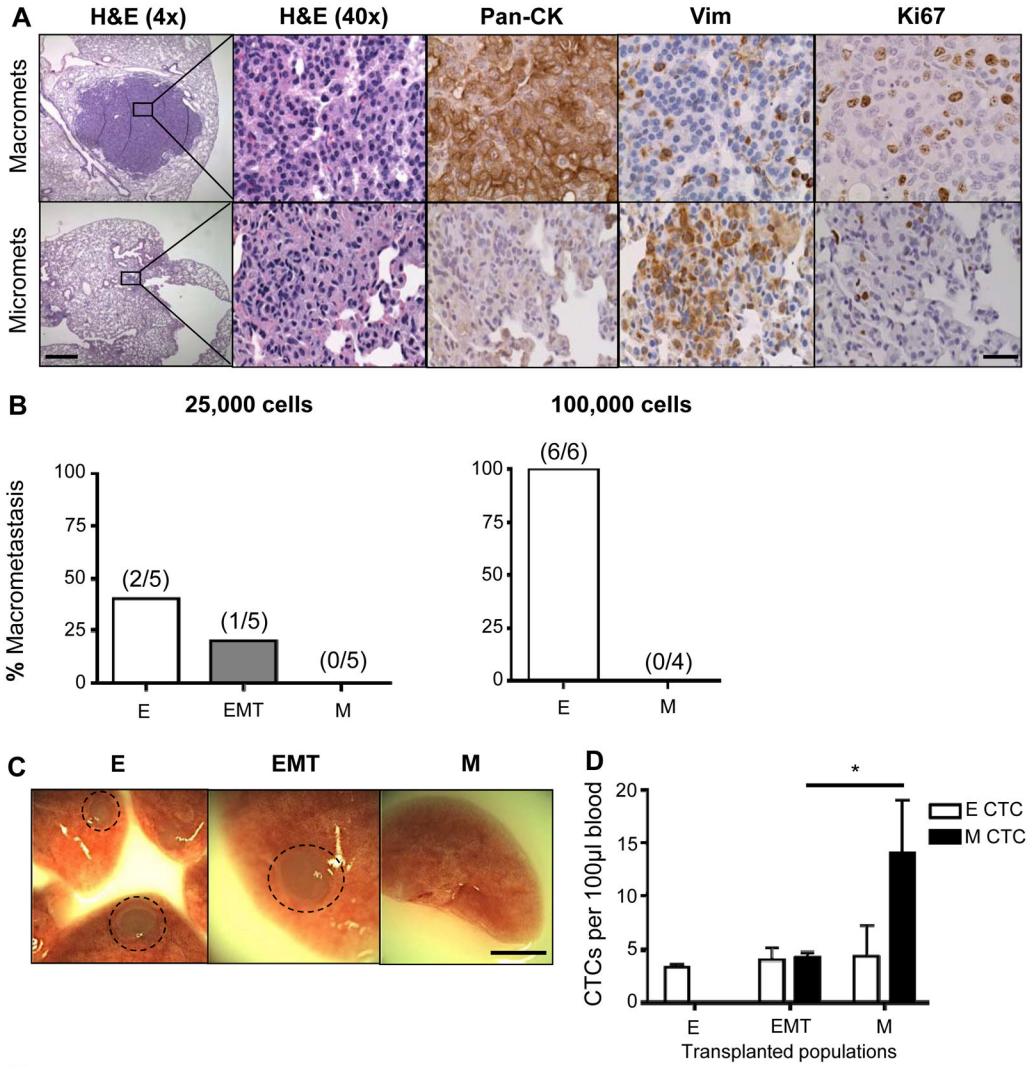

E

	Epithelial	EMT-like	Mesenchymal
EMT gene expression		++	++++
Sphere Formation	++	++++	+
Stemness gene expression		++	+++
Proliferation	+++	+++	+
Invasive capacity	+	++	++++
Tumor-initiating capacity	+	+++	++++
Metastatic Seeding capacity	++	+	

Figure 6.

Epithelial tumor cells have enhanced metastatic seeding potential. **A**, IHC analysis of epithelial (Pan-CK), mesenchymal (Vim), and proliferation (Ki67) markers in micrometastases (micromets) and macrometastases (macromets) in primary *CPKV* lungs (18 weeks). Low magnification bar, 500 µm; high magnification bar, 50 µm. **B**, Percent of macrometastatic lesions in the lungs of *NSG* mice 16 weeks after intravenous transplantation of either 25,000 or 100,000 epithelial, EMT, or mesenchymal tumor cells from *CPKV* prostates (10–12 weeks). **C**, Whole-mount images of lungs isolated from *NSG* mice

transplanted with 25,000 epithelial, EMT, or mesenchymal tumor cells from *CPKV* prostates (10–12 weeks). Circle, macrometastases. Bar, 4 mm. **D**, *NSG* mice transplanted intravenously with mesenchymal tumor cells (25,000) from *CPKV* prostates (10–12 weeks) contained a significantly higher number of CTCs persisting in the bloodstream compared to mice transplanted with either epithelial or EMT tumor cells 16 weeks post-transplantation. **E**, Table summarizing the characteristics of epithelial, EMT, and mesenchymal tumor cells isolated from *CPKV* prostates. Data in D are represented as mean ± SEM. *, $P < 0.05$